ISSN 1674-1056
http://cpb.iphy.ac.cn
http://iopscience.iop.org/cpb
中国物理 B
Chinese Physics
中国物理 Chinese Physics B

Thermodynamic and structural properties of polystyrene/C_{60} composites: A molecular dynamics study

Junsheng Yang(杨俊升), Ziliang Zhu(朱子亮), Duohui Huang(黄多辉), Qilong Cao(曹启龙)
Citation: Chin. Phys. B . 2020, 29(2): 023104 . **doi:** 10.1088/1674-1056/ab6312
Journal homepage: http://cpb.iphy.ac.cn; http://iopscience.iop.org/cpb

What follows is a list of articles you may be interested in

Elastic properties of anatase titanium dioxide nanotubes: A molecular dynamics study

Kang Yang(杨康), Liang Yang(杨亮), Chang-Zhi Ai(艾长智), Zhao Wang(王赵), Shi-Wei Lin(林仕伟)
Chin. Phys. B . 2019, 28(10): 103102 . **doi:** 10.1088/1674-1056/ab3da2

Ethylene glycol solution-induced DNA conformational transitions

Nan Zhang(张楠), Ming-Ru Li(李明儒), Feng-Shou Zhang(张丰收)
Chin. Phys. B . 2018, 27(11): 113102 . **doi:** 10.1088/1674-1056/27/11/113102

A simulation study of water property changes using geometrical alteration in SPC/E

Ming-Ru Li(李明儒), Nan Zhang(张楠), Feng-Shou Zhang(张丰收)
Chin. Phys. B . 2018, 27(8): 083103 . **doi:** 10.1088/1674-1056/27/8/083103

Diffusion behavior of hydrogen isotopes in tungsten revisited by molecular dynamics simulations

Mingjie Qiu(丘明杰), Lei Zhai(翟磊), Jiechao Cui(崔节超), Baoqin Fu(付宝勤), Min Li(李敏), Qing Hou(侯氢)
Chin. Phys. B . 2018, 27(7): 073103 . **doi:** 10.1088/1674-1056/27/7/073103

Anisotropic self-diffusion of fluorinated poly(methacrylate) in metal-organic frameworks assessed with molecular dynamics simulation

Tao Lu(鲁桃), Biao Xu(徐彪), Fei-Hong Ye(叶飞宏), Xin-Hui Zhou(周馨慧), Yun-Qing Lu(陆云清), Jin Wang(王瑾)
Chin. Phys. B . 2017, 26(12): 123104 . **doi:** 10.1088/1674-1056/26/12/123104

Thermodynamic and structural properties of polystyrene/C_{60} composites: A molecular dynamics study*

Junsheng Yang(杨俊升)[1,†], Ziliang Zhu(朱子亮)[2], Duohui Huang(黄多辉)[1], and Qilong Cao(曹启龙)[1,‡]

[1] *Computational Physics Key Laboratory of Sichuan Province, Yibin University, Yibin* 644000, *China*
[2] *Weifang University of Science and Technology, Shouguang* 262700, *China*

(Received 11 September 2019; revised manuscript received 29 November 2019; accepted manuscript online 18 December 2019)

To tailor properties of polymer composites are very important for their applications. Very small concentrations of nanoparticles can significantly alter their physical characteristics. In this work, molecular dynamics simulations are performed to study the thermodynamic and structural properties of polystyrene/C_{60} (PS/C_{60}) composites. The calculated densities, glass transition temperatures, and coefficient of thermal expansion of the bulk PS are in agreement with the experimental data available, implying that our calculations are reasonable. We find that the glass transition temperature T_g increases accordingly with an added concentration of C_{60} for PS/C_{60} composites. However, the self-diffusion coefficient D decreases with increase of addition of C_{60}. For the volumetric coefficients of thermal expansion (CTE) of bulk PS and PS/C_{60} composites, it can be seen that the CTE increases with increasing content of C_{60} above T_g (rubbery region). However, the CTE decreases with increasing content of C_{60} below T_g (glassy region).

Keywords: polystyrene/C_{60} composites, molecular dynamics, glass transition, diffusion

PACS: 31.15.xv, 65.80.–g, 65.40.De **DOI:** 10.1088/1674-1056/ab6312

1. Introduction

Polymer nanocomposites (PNCs) have received considerable attention because they can be added to polymer matrixes to alter their thermal-mechanical and structural properties without affecting their chemical features.[1] Nanoparticles, such as nanotubes[2] and fullerenes,[3] gold nanoparticles,[4] silica nanoparticles,[5] and others,[6] have been used in PNCs over a century. This is due to the key factors in tailoring the properties of polymeric materials, namely, the structure and diffusion of polymer chains are dependent on the foreign surface.[7–10] Therefore, we need to know more about the thermodynamic and diffusion properties of polymer systems which are filled with nanoparticlas.

Interfacial interactions between nanoparticles and polymers play important roles in glass transition of PNCs. The glass transition temperature (T_g) of a polymer matrix can be enhanced by addition of nanoparticles, which is due to the fact that the mobility of polymer chains is limited by the nanoparticles. However, two different views emerged for the change of T_g of PNCs in recent experiments. Oh *et al.* reported that PNCs containing $AuPS_{10}$ nanoparticles can exhibit substantially lower T_g values than that of bulk polystyrene (PS).[4] In contrast, T_g of PS/C_{60} composites is higher than bulk PS.[3] Recent experimental results also show that PNCs containing silica nanoparticles exhibit two T_g's. One is associated with the week interaction between nanoparticles and polymer chains far from the nanoparticles. The other is related to the strong interaction between the nanoparticles and polymer chains nearby the nanoparticles.[1] For systems of PNCs, recent experimental results exhibit that the increase of T_g is mainly due to low mobility of polymer chains in the nanocomposites. From the concept of free volume, the molecular motion is relatively easy because the polymer chains have a larger free volume at the liquid state than melts. With the infusion of nanoparticles, the free volume can be reduced until there would not be enough free space to allow molecular translation of motion.[11]

Nanoparticles play an important role in thermal expansion and diffusion properties of a polymer matrix. For example, the recent simulated results display that polymer chains in the vicinity of a nanoparticle are more immobilized than those in the outermost region.[3] Wei *et al.*[12] demonstrated that the diffusion coefficient of polymer chains is profoundly increased with the presence of carbon nanotubes (CNTs). Their results also prove that the coefficient of thermal expansion (CTE) of polymer chains can be enhanced with addition of CNTs. The composites have a fixed volume and exclude the occupancy of the polymer chains. The increased CTE of the composites is attributed to the increase in the excluded volume of the embedded CNTs.

To improve the efficiency of experiment in synthesis and optimization of material properties, computer simulations are

*Project supported by the National Natural Science Foundation of China (Grant No. 11704329), the Scientific Research Fund of Sichuan Provincial Education Department of China (Grant No. 15ZB293), the Pre-Research Project of Yibin University of China (Grant No. 2019YY06), and the Open Research Fund of Computational Physics Key Laboratory of Sichuan Province at Yibin University of China (Grant No. JSWL2014KF02).

†Corresponding author. E-mail: yangjunsheng2005@163.com
‡Corresponding author. E-mail: qlcao@mail.ustc.edu.cn

© 2020 Chinese Physical Society and IOP Publishing Ltd

an effective tool to solve this problem. Molecular dynamics (MD) simulations are often used to predict properties of polymeric materials and local interaction problems of material interfaces.[13–16] The authors of Refs. [13–19] found the same tendency that smaller nanoparticles were more appropriate to increase mechanical performance of PNCs by performing MD simulations. Yang *et al.*[17] have reported that the specific monomer structure plays an important role in determining the strength of interaction between CNTs and polymers. If we want to design favorable microscopic and macroscopic structures of PNC materials, we need to know more about the molecular mechanism of PNC systems.

In this work, MD simulations are performed to study the glass transition and diffusion properties of PS/C_{60} nanocomposites. Since the physical properties of PNCs are directly influenced by the interfacial interaction between the nanoparticles and polymers, the present simulation emphasizes the examination of effects of nanoparticle loading and temperatures.

2. Model and simulation method

For all the simulation processes, the commercially available MD simulation package Materials Studio is used in this work. The second-generation COMPASS (condensed-phase optimized molecular potentials for atomistic simulation studies) force field has been used to describe the inter- and intra-atomic interactions of PS/C_{60} systems.[18] The COMPASS force field is often used to predict the properties of the polymer system, which is due to its high accuracy. The recent simulation results have shown that the densities, coefficients of thermal expansion, and the glass transition temperature agree with the available experimental data for thermoset polymer networks using the COMPASS force field.[19] Wu *et al.*[20] and Tack *et al.*[21] also found that the COMPASS force field for predicting the properties of polymer networks is better than that of cff91 and DREIDING force fields. In our previous work, the COMPASS force field was successfully used in predicting the density and interfacial interaction properties of the Nylon 6 and CNT composites.[22] The force field potential can be expressed as follows:[23]

$$E_{\text{total}} = E_{\text{valence}} + E_{\text{cross-term}} + E_{\text{nonbond}}, \tag{1}$$

where the first term E_{valence} is the valence energy. The second term $E_{\text{cross-term}}$ is the cross-term interacting energy. The third term E_{nonbond} is the nonbond interacting energy. The detail about every term is expressed as follows:

$$\begin{aligned} E_{\text{valence}} = {} & \sum_b [K_2(b-b_0)^2 + K_3(b-b_0)^3 + K_4(b-b_0)^4] \\ & + \sum_\theta [H_2(\theta-\theta_0)^2 + H_3(\theta-\theta_0)^3 + H_4(\theta-\theta_0)^4] \\ & + \sum_\varphi [V_1[1-\cos(\varphi-\varphi_1^0)] + V_2[1-\cos(2\varphi-\varphi_2^0)] \\ & + V_3[1-\cos(3\varphi-\varphi_3^0)]] + \sum_\chi K_\chi \chi^2 + E_{\text{UB}}, \end{aligned} \tag{2}$$

$$\begin{aligned} E_{\text{cross-term}} = {} & \sum_b \sum_{b'} F_{bb'}(b-b_0)(b'-b_0') \\ & + \sum_\theta \sum_{\theta'} F_{\theta\theta'}(\theta-\theta_0)(\theta'-\theta_0') \\ & + \sum_b \sum_\theta F_{b\theta}(b-b_0)(\theta-\theta_0) \\ & + \sum_b \sum_\varphi F_{b\varphi}(b-b_0)[V_1\cos\varphi + V_2\cos(2\varphi) + V_3\cos(3\varphi)] \\ & + \sum_{b'} \sum_\varphi F_{b'\varphi}(b'-b_0')(b'-b_0')[F_1\cos\varphi + F_2\cos(2\varphi) + F_3\cos(3\varphi)] \\ & + \sum_\theta \sum_\varphi F_{\theta\varphi}(\theta-\theta_0)[V_1\cos\varphi + V_2\cos(2\varphi) + V_3\cos(3\varphi)] \\ & + \sum_\varphi \sum_\theta \sum_{\theta'} K_{\varphi\theta\theta'}\cos\varphi(\theta-\theta_0)\times(\theta'-\theta_0'), \end{aligned} \tag{3}$$

$$E_{\text{nonbond}} = \sum_{i>j}\left[\frac{A_{ij}}{r_{ij}^9} - \frac{B_{ij}}{r_{ij}^6}\right] + \sum_{i>j}\frac{q_i q_j}{\varepsilon r_{ij}}, \tag{4}$$

where b and b' are the bond lengths, θ is the two-bond angle, φ is the dihedral torsion angle, χ is the out of plane angle, q is the atomic charge, ε is the dielectric constant, r_{ij} is the i–j atomic separation distance; b_0, K_i (i = 2–4), θ_0, H_i (i = 2–4), φ_i^0 (i = 2–4), V_i (i = 1–3), $F_{bb'}$, b_0', $F_{\theta\theta'}$, θ_0', $F_{b\theta}$, $F_{b\varphi}$, $F_{b'\theta}$, F_i (i = 1–3), $F_{\theta\varphi}$, $K_{\varphi\theta\theta'}$, A_{ij}, and B_{ij} are the system-dependent parameters. The time step is 1 fs and the cutoff distance is 9.5 Å for all calculations. The Anderson method[24] is applied to control the temperature in all the calculations.

The experimental results have shown that C_{60} plays a key role in the glass translation and the mechanical properties of the polymer/C_{60}.[3,25] Kropka *et al.*[3] shown that the PS/C_{60} and poly(methyl methacry-late) (PMMA)/C_{60} composites exhibit an increase in their "bulk" T_g. Song *et al.*[25] demonstrated that polymer/C_{60} nanocomposites possess good mechanical properties. Figure 1 displays the structure of PS and C_{60}. The single PS chain is made up of 10 $C_2H_3(C_6H_6)$ groups. In order to investigate the thermal properties of the polymer system with the addition of nanoparticles, C_{60} is distributed uniformly in the PS matrix (Fig. 2(b)). The periodic boundary condition is used in our simulations. For the bulk PS system, the initial cell size is 4.073 nm × 4.073 nm × 4.073 nm (total 6480 atoms in the unit cell, as shown in Fig. 2(a)). The density is about 1.03 g/cm^3 for the pristine PS at 300 K, which is close to the experimental values (1.04–1.065 g/cm^3).[26] This implies that the model of the present PS system is reasonable and the computational policy is acceptable. For the PS/C_{60} composites, three different concentration ratios of C_{60} in the PS matrix (1.7 wt%, 3.3 wt%, and 4.9 wt%, respectively) are studied in the present calculations. The three different concentration ratios of C_{60} are represented as PS/C_{60}-1, PS/C_{60}-2, and PS/C_{60}-3 in the succeeding discussions.

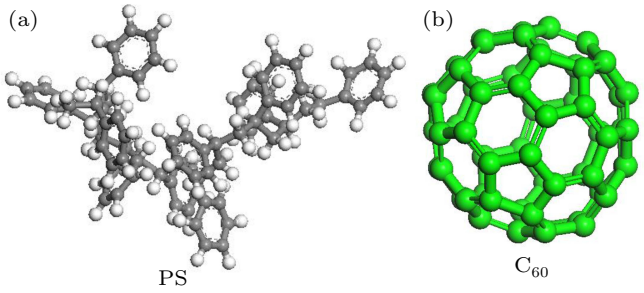


Fig. 1. Molecular model of (a) PS and (b) C_{60}.

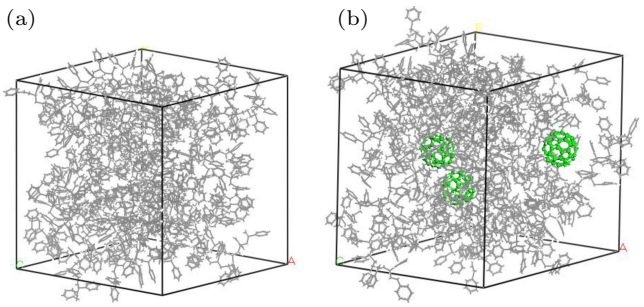


Fig. 2. (a) Bulk PS and (b) PS/C_{60} nanocomposite systems.

Firstly, the MD with NPT ensemble is performed for 200 ps to make the studied systems reach their equilibrium at 500 K and 1 atm. Figure 3 shows the evolutions of the difference in total energy between structure and initial structure of the three systems. It is observed that the energies quickly equilibrate in less than 50 ps and then continues to fluctuate around the equilibrium value, which implies that the simulation time of 200 ps is long enough for the systems to reach relax state. The method is the same as that used in our previous works.[22,27] Then, the systems are gradually cooled to 300 K with the quenching rates of 20 K/100 ps. The effect of the rate of quenching has been provided in Fig. 4. From the following figures, it can been seen that the changes of density and glass transition temperature are weak under the two quenching rates for pure PS and PS/C_{60}-3 systems, which means that the 100 ps is long enough for the systems reaching relaxation states when the systems at the target temperature.

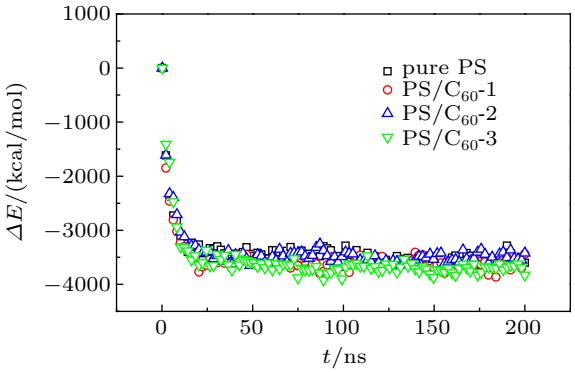


Fig. 3. The evolutions of the potential energy difference between the structure and initial structure for the three systems.

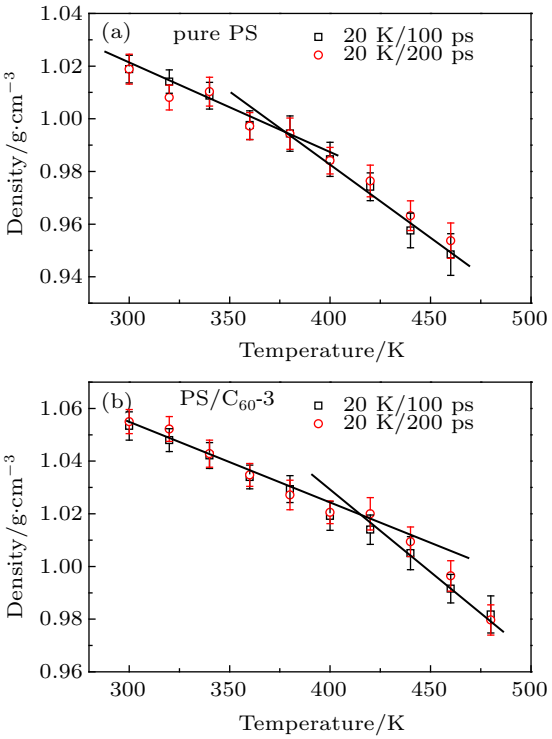


Fig. 4. The evolutions of the density and glass transition temperature for (a) pure PS and (b) PS/C_{60}-3 systems.

3. Results and discussion

3.1. Glass transition and thermal expansion properties of bulk PS and PS/C_{60} composites

3.1.1. Density of bulk PS and PS/C_{60} composites

Figure 5 displays the density as a function of temperature for the bulk PS and PS/C_{60} composites. For the bulk PS system, the density (1.03 g/cm^3) is consistent with the experimental values (1.04–1.065 g/cm^3) at room temperature (T = 300 K).[26] The density of PS/C_{60} composite systems is also shown in Fig. 4. As is expected, the density of the PS/C_{60} system is strongly enhanced with the increasing concentration of C_{60} in the whole temperature range. This is due to the stronger interactions of inter-chains in the PS/C_{60} system. Teh *et al.*[28] have investigated the interaction between

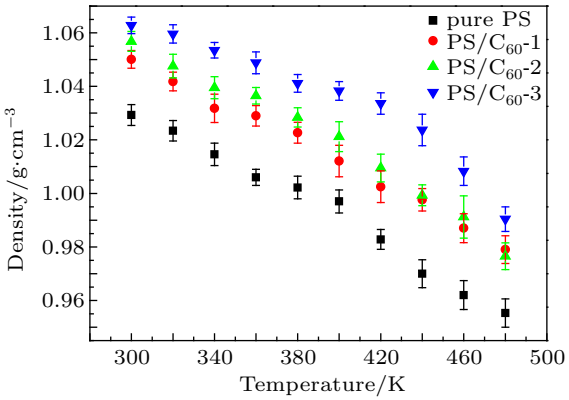


Fig. 5. Density as a function of temperature for bulk PS and PS/C_{60} composites.

the C_{60} and each monomer, and the results demonstrated that the polymer composites have a smaller distance between C_{60} and functional group, and have stronger intermolecular interactions than the pure polymer melts. For the PS consisting of styrene monomer, the first principle results have proved that the binding energy between C_{60} and styrene is stronger than that between C_{60} and other functional groups, which implies that the PS has the stronger binding energy with C_{60}.

3.1.2. Glass transition of bulk PS and PS/C_{60} composites

The results of the glass translation of bulk PS and PS/C_{60}-3 composites are presented in Fig. 6. From Fig. 6, the specific volume continuously increases with increasing temperature. Obviously, the change of volume possesses good linearity with temperature in high and low-temperature regions. Because of the strong interfacial interaction between C_{60} and PS, the specific volume continuously decreases with increasing C_{60} nanoparticales in the whole temperature range. The low and high temperature regions correspond to the glassy and rubbery regions, respectively. Glass transition temperatures are determined at the point of the change in the slope (represented by the intersection of the solid lines in Fig. 6). The glass transition temperature was enhanced with the addition of C_{60}. The current T_g value is about 372 K for bulk PS (see Fig. 6), which is consistent with the experimental report (373 K).[26] This implies that the current cooling rate and method are valid to determine T_g of the PS systems. The T_g is about 420 K for the PS/C_{60}-3 system, increased by about 40 K compared with the bulk PS system, and the value is consistent with the previous MD simulations conducted on a similar system.[22] However, the value is larger than the experimental data,[29] which is related with the force field. However, the tendency of T_g of PS/C_{60} agrees with the experimental data.

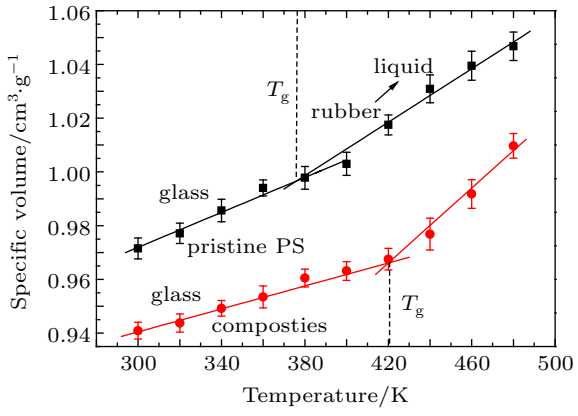


Fig. 6. Glass transition temperatures for bulk PS and PS/C_{60}-3 composites.

In general, T_g is associated with the mobility of the chains. The experimental and theoretical results have demonstrated that the increasing T_g represents the strong interactions between the particle and polymer chains, while the decreasing T_g is due to the weak interactions. The increasing T_g for the PS/C_{60} system upon the addition of C_{60} is interpreted to the result of the strong interactions between the C_{60} and PS chains, and the interactions reduce the molecular mobility and the flexibility of the polymer chain nearby the C_{60} nanoparticles.

3.1.3. Volumetric coefficient of thermal expansion of bulk PS and PS/C_{60} composites

The increasing specific volumes of the bulk PS and the composite with increasing temperature indicate the thermal expansions of the composites. The slopes of the curves give the volumetric coefficient of thermal expansion (CTE) as $(\frac{1}{V})(\frac{\partial V}{\partial T})$ in glassy and rubbery regions,[12] respectively. Figure 7 shows that the CTE increases with increasing content of C_{60} in the region of above T_g (rubbery region). However, the CTE decreases with increasing content of C_{60} below T_g (glassy region). The experimental values for bulk PS at glassy and rubbery states are also shown in Fig. 7. The CTE value obtained from our simulations for bulk PS is in agreement with the experimental data in the rubbery region. The CTE value of bulk PS is slightly larger than the experimental data in the glassy region.

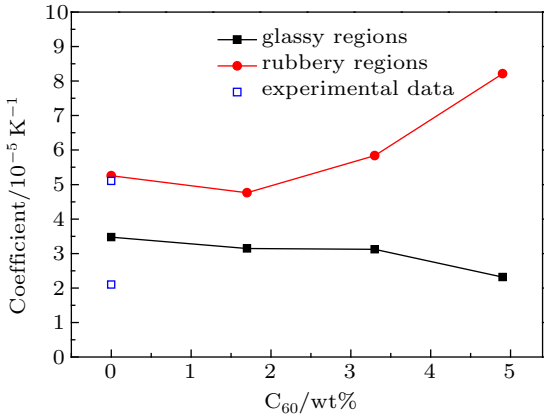


Fig. 7. Volumetric coefficients of thermal expansion for the glassy and rubbery regions.

3.2. Diffusion properties of PS chains in bulk PS and PS/C_{60} composites

Molecular mobility and flexibility are influenced by the temperature and the content of nanoparticles. The molecular mobility and flexibility of PS chains can be directly described by the self-diffusion coefficient (D) of PS chains. The self-diffusion coefficients are calculated from the mean squared displacement (MSD), which is defined as follows:[30]

$$D = \lim_{t\to\infty} \frac{1}{6t} \left\langle [r(t+t_0) - r(t_0)]^2 \right\rangle, \tag{5}$$

where $r(t_0)$ is the initial coordinate and $r(t+t_0)$ the position of chain atoms after a time t. Figure 8(a) shows the MSD of

PS chains as a function of time for the bulk PS and PS/C_{60} composite systems at the temperature of 480 K, respectively. Obviously, the curves of MSD versus time are linear. The diffusion coefficient D is the slop of the MSD to time t.

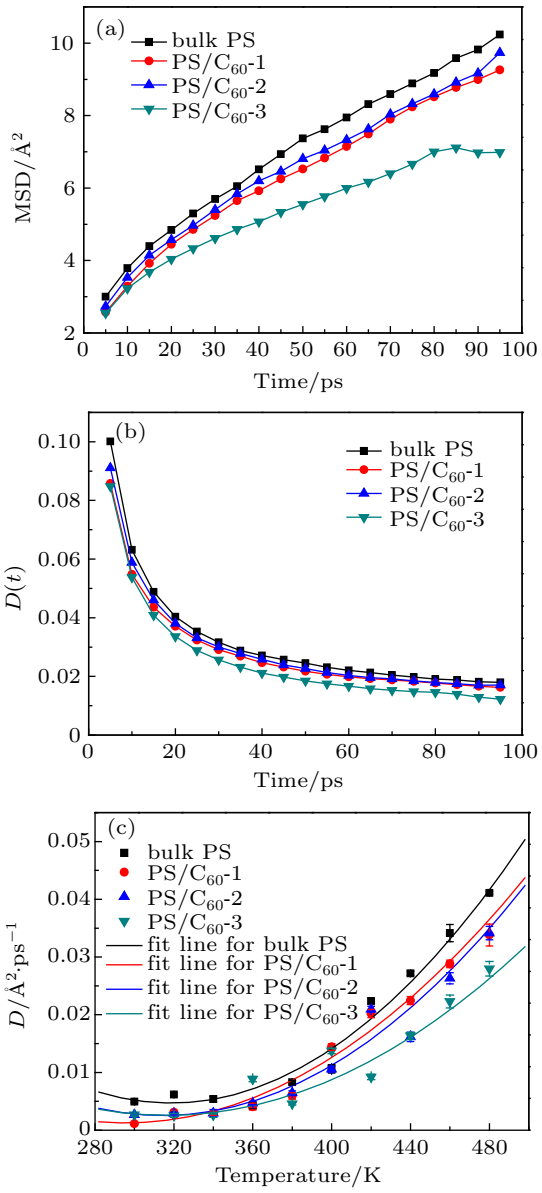


Fig. 8. (a) The mean-square displacement (MSD) as a function of time for bulk PS and PS/C_{60} composites under the temperature of 480 K. (b) The diffusion coefficient $D(t)$ as a function of evolution time for bulk PS and PS/C_{60} composites under the temperature of 480 K. (c) The diffusion coefficient $D(t)$ as a function of temperature for bulk PS and PS/C_{60} composites.

Figure 8(c) displays the D of PS chains as a function of temperature for bulk PS, PS/C_{60}-1, PS/C_{60}-2, and PS/C_{60}-3 systems, respectively. The strong interfacial interaction will inflect to the mobility and the flexibility of PS chains nearby the C_{60} nanoparticles. Obviously, bulk PS chains have a larger D than PS chains in PS/C_{60} composites in the whole temperature range. The D continuously decreases with increasing content of C_{60}. However, Harmandaris *et al.*[31] have reported that the D is not a constant in all the cases and the time-dependent diffusion coefficient $D(t)$ is more proper to describe the properties. Therefore, the time-dependent diffusion coefficients $D(t)$ of PS chains are calculated by the equation $D(t) = \langle r(t)^2 \rangle / (6t)$.[25] The results are presented in Fig. 8(b). Obviously, $D(t)$ has a sudden drop in a very short period of time. At later time, the $D(t)$ is found to reach a plateau value.

3.3. Radius of gyration of PS in bulk PS and PS/C_{60} composites

To better understand the conformational change of PS chains in bulk PS and PS/C_{60} composites, the radius of gyration (R_g) of the chains as functions of temperature and concentration of C_{60} is displayed in Fig. 9.

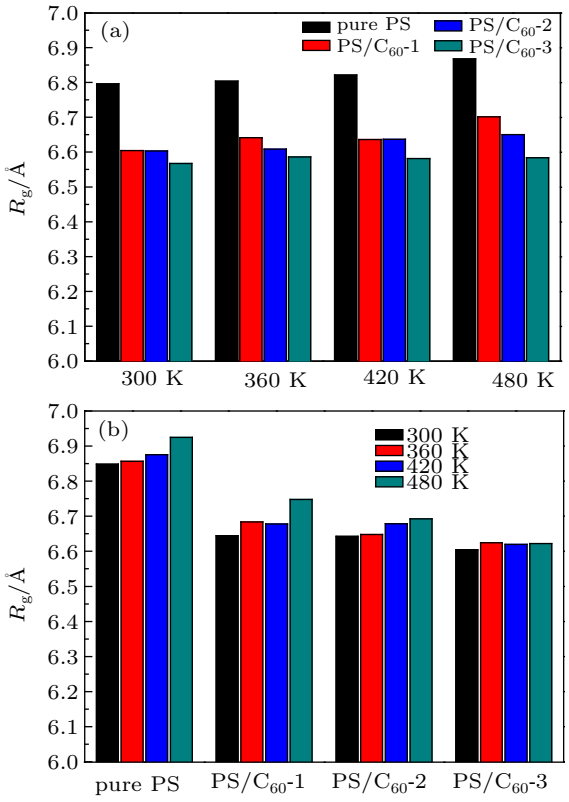


Fig. 9. The radius of gyration of PS chains in bulk PS and PS-C_{60} composites.

Obviously, the R_g of PS chains in the bulk PS system is larger than that in the composites under different temperatures (see Fig. 9(a)). This is due to the fact that the strong interfacial interaction plays an important role in the conformation of the chains. Thus, the R_g of PS chains decreases with increasing content of C_{60} nanoparticles. To determine the effect of the temperature, Fig. 9(b) presents the R_g of PS chains in bulk PS and in the composites under different temperatures. From Fig. 9(b), it can be seen that the difference of the R_g of PS chains between the lower and higher temperatures is very little with the increase of the content of C_{60}, indicating that the temperature has little effect on the R_g of PS chains in the composites. This implies that the structure of the PS chains

is influenced by the temperature, but the strong interfacial interaction of polymer-nanoparticle can assuage the effect of the temperature.

3.4. Interaction energy between C_{60} and PS chains

To investigate the binding strength of interfacial interaction, the interfacial binding energy (IBE) between PS and C_{60} is calculated. Generally, IBE is estimated by the difference between the potential energy of the composite system and the potential energy for the polymer matrix and the corresponding C_{60} as follows:[25]

$$\Delta E = E_{\text{total}} - (E_{C_{60}} + E_{\text{polymer}}), \tag{6}$$

where E_{total} is the total potential energy of the system, $E_{C_{60}}$ is the total potential energy of C_{60} without the polymer, and the E_{polymer} is the total potential energy of the PS chains without C_{60}.

Figure 10 shows the IBE between PS and C_{60} for the PS/C_{60}-1, PS/C_{60}-2, and PS/C_{60}-3, respectively. The results from the first principle show that the styrene exhibits a relatively high binding energy with C_{60}, and IBE is found to be 3.21 kcal/mol, which is larger than that of C_{60} with other monomers. We find that IBE of C_{60} and PS is strongly enhanced by increasing concentration of C_{60}. The origin of the higher IBE in the composites is explained as follows. PS is able to interact with C_{60} via π–π interactions between the curved π surface of the C_{60} cage and the flat π surface of the phenyl ring of PS. In addition, the distance between C_{60} and PS is also relatively small, ~2.63 Å, indicating the strong interaction between the nanoparticle and the PS. From Fig. 10, it can be seen that the energy difference between the lower temperature and the higher temperature is very little for the PS/C_{60}-1, which indicates that the temperature has little effect on IBE of the nanocomposites with lower concentration of C_{60}. On the contrary, for the nanocomposite systems containing the C_{60} with higher concentration of C_{60}, the energy difference between the lower temperature and higher temperature is obvious. This implies that the IBE depends on both the concentration of the nanoparticles and the temperature of the system.

Combining the change of glass transition and diffusion of polymer chains, as seen in Fig. 10(b), we can realize that the mobility of the polymer chains is related with IBE between PS chains and C_{60} in the interfacial region, and the diffusion self-coefficients of PS chains decreases with increasing concentration of C_{60} in the interfacial region. Meanwhile, the T_g is associated with the interfacial interaction and mobility of PS chains, therefore the glass transition temperature increases with the addition of C_{60} in bulk PS melts.

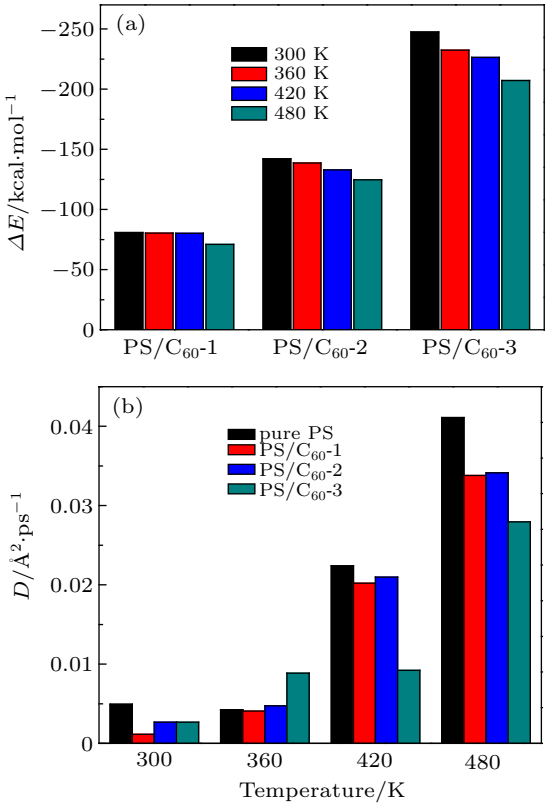


Fig. 10. (a) The interfacial interaction binding energy between PS and C_{60} with different concentrations of C_{60}. (b) The diffusion coefficient D for bulk PS and PS chains in the composites at different temperatures.

4. Conclusions

In this work, MD simulations are performed to predict the physical properties of the bulk PS and PS/C_{60} composites. The simulations demonstrate that the thermal expansion and diffusion properties of the PS system are effectively improved by addition of C_{60}. The density, glass transition temperature, and volumetric coefficients of thermal expansion are in good agreement with the experimental data. The present MD results have displayed that the densities and the glass translation temperatures of the composite systems are strongly enhanced with the increasing concentration of C_{60}. However, the self-diffusion coefficients of the PS chains continuously decrease with the increasing content of C_{60}. We also find that the self-diffusion coefficients of the PS chains are more diffusive at temperature above T_g. The increase in the T_g and the decrease in the self-diffusion coefficients upon the addition of C_{60} are interpreted to the result of the presence of a strong interaction between the C_{60} and PS chains, as this interaction reduces the molecular mobility and the flexibility of the polymer chain nearby the C_{60} fullerenes. For the volumetric coefficients of thermal expansion of bulk PS and composites cases, the simulations results show that above T_g (rubbery region), the CTE increases with the increasing content of C_{60}. However, the CTE decreases with the increasing content of C_{60} below T_g (glassy region). These findings have potential applications in

polymer composite processing, coating, and printing.

References

[1] Tsagaropoulos G and Eisenberg A 1995 *Macromolecules* **28** 396
[2] Bing L, Lingyu L, Bingbing W and Li C Y 2009 *Nat. Nanotechnol.* **4** 358
[3] Kropka J M, Garcia S V and Green P F 2008 *Nano Lett.* **8** 1061
[4] Oh H and Green P F 2009 *Nat. Mater.* **8** 139
[5] Ndoro T V M, Voyiatzis E, Ghanbari A, Theodorou D N, Böhm M C and Müllerplathe F 2011 *Macromolecules* **44** 2316
[6] Cho J, Joshi M S and Sun C T 2006 *Compos. Sci. & Technol.* **66** 1941
[7] Yan C, Horn R M V, Tsai C C, Graham M J, Jeong K U, Wang B, Auriemma F, Rosa C D, Lotz B and Cheng S Z D 2009 *Macromolecules* **42** 4758
[8] Sun Y, Li H, Huang Y, Chen E, Zhao L, Gan Z and Yan S 2006 *Polymer* **47** 2455
[9] Cheng S, Hu W, Yu M and Yan S 2007 *Polymer* **48** 4264
[10] Chang H, Zhang J, Lin L I, Wang Z, Yang C, Takahashi I, Ozaki Y and Yan S 2010 *Macromolecules* **43** 362
[11] Mahfuz H, Adnan A, Rangari V K, Hasan M M, Jeelani S, Wright W J and Deteresa S J 2006 *Appl. Phys. Lett.* **88** 083119
[12] Wei C, Srivastava D and Cho K 2002 *Nano Lett.* **2** 647
[13] Yang S, Choi J and Cho M 2012 *Acs Appl. Mater. & Interfaces* **4** 4792
[14] Yang S and Cho M 2009 *Appl. Phys. Lett.* **94** 223104
[15] Yu S, Yang S and Cho M 2009 *Polymer* **50** 945
[16] Liu J, Wu S, Zhang L, Wang W and Cao D 2011 *Phys. Chem. Chem. Phys. Pccp* **13** 518
[17] Yang M J, Koutsos V and Zaiser M 2005 *J. Phys. Chem. B* **109** 10009
[18] Sun H 1998 *J. Phys. Chem. B* **102** 7338
[19] Stevens M J 2001 *Macromolecules* **34** 2710
[20] Wu C and Xu W 2006 *Polymer* **47** 6004
[21] Tack J L and Ford D M 2008 *J. Mol. Graph. & Modell.* **26** 1269
[22] Yang J S, Yang C L, Wang M S, Chen B D and Ma X G 2012 *Rsc Adv.* **2** 2836
[23] Grujicic M, Cao G and Roy W N 2004 *Appl. Surf. Sci.* **227** 349
[24] Andersena H C 1983 *J. Comput. Phys.* **52** 24
[25] Song T, Goh S H and Lee S Y 2003 *Polymer* **44** 2563
[26] Brandrup J, Immergut E H, Grulke E A, Abe A and Bloch D R 1999 *Polymer Handbook* (New York: Wiley) Vol. 89
[27] Yang J S, Huang D H, Cao Q L, Li Q, Wang L Z and Wang F H 2013 *Chin. Phys. B* **22** 098101
[28] Teh S L, Linton D, Sumpter B and Dadmun M D 2011 *Macromolecules* **44** 7737
[29] Sanz A, Wong H C, Nedoma A J, Douglas J F and Cabral J T 2015 *Polymer* **68** 47
[30] Yang J S, Yang C L, Wang M S, Chen B D and Ma X G 2011 *Phys. Chem. Chem. Phys.* **13** 15476
[31] Harmandaris V A and Kremer K 2009 *Macromolecules* **42** 791